AD-A051 453 OAKLAND UNIV ROCHESTER MICH SCHOOL OF ENGINEERING F/G 13/13
OPTIMIZATION OF GEOMETRIC DISCONTINUITIES IN STRESS FIELDS.(U)
MAR 78 A J DURELLI, K BROWN, P YEE N00014-76-C-0487
UNCLASSIFIED 46 NL

OF
AD
A051453

END
DATE
FILMED
4-78
DDC

OPTIMIZATION OF GEOMETRIC DISCONTINUITIES IN STRESS FIELDS

BY

A. J. DURELLI, K. BROWN AND P. YEE

SPONSORED BY

OFFICE OF NAVAL RESEARCH
DEPARTMENT OF THE NAVY
WASHINGTON, D.C. 20025

ON

CONTRACT No. N00014-76-C-0487
O.U. PROJECT No. 31414-24
REPORT No. 46

AND

NATIONAL SCIENCE FOUNDATION
WASHINGTON, D.C. 20550

ON

GRANT No. ENG77-07974
O.U. PROJECT No. 32110-18

SCHOOL OF ENGINEERING
OAKLAND UNIVERSITY
ROCHESTER, MICHIGAN 48063

MARCH 1978

OPTIMIZATION OF GEOMETRIC DISCONTINUITIES IN STRESS FIELDS

by

A. J. Durelli, K. Brown and P. Yee

Sponsored by

Office of Naval Research
Department of the Navy
Washington, D.C. 20025

on

Contract No. N00014-76-C-0487
O.U. Project No. 31414-24
Report No. 46

and

National Science Foundation
Washington, D.C. 20550

on

Grant No. ENG77-07974
O.U. Project No. 32110-18

School of Engineering
Oakland University
Rochester, Michigan 48063

March 1978

Abstract

The ideal boundary of a discontinuity is defined as that boundary along which there is no stress concentration. Photoelastically an isochromatic coincides with the ideal boundary. This property is used to develop experimentally ideal boundaries for some cases of technological interest. The concept of "coefficient of efficiency" is introduced to evaluate the degree of optimization. The procedure to idealize boundaries is illustrated for the two cases of the circular tube and of the perforated rectangular plate, with prescribed functional restraints and a particular criterion for failure. An ideal design of the inside boundary of the tube is developed which decreases its maximum stress by 25%, at the time it also decreases its weight by 10%. The efficiency coefficient is increased from 0.59 to 0.95. Tests with a brittle material show an increase in strength of 20%. An ideal design of the boundary of the hole in the plate reduces the maximum stresses by 26% and increases the coefficient of efficiency from 0.54 to 0.90.

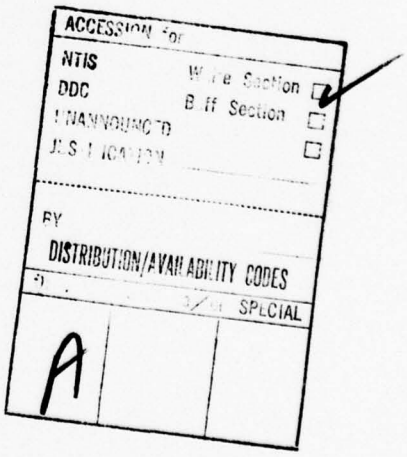

Previous Technical Reports to the Office of Naval Research

1. A. J. Durelli, "Development of Experimental Stress Analysis Methods to Determine Stresses and Strains in Solid Propellant Grains"--June 1962.
   Developments in the manufacturing of grain-propellant models are reported. Two methods are given: a) cementing routed layers and b) casting.

2. A. J. Durelli and V. J. Parks, "New Method to Determine Restrained Shrinkage Stresses in Propellant Grain Models"--October 1962.
   The birefringence exhibited in the curing process of a partially restrained polyurethane rubber is used to determine the stress associated with restrained shrinkage in models of solid propellant grains partially bonded to the case.

3. A. J. Durelli, "Recent Advances in the Application of Photoelasticity in the Missile Industry"--October 1962.
   Two- and three-dimensional photoelastic analysis of grains loaded by pressure and by temperature are presented. Some applications to the optimization of fillet contours and to the redesign of case joints are also included.

4. A. J. Durelli and V. J. Parks, "Experimental Solution of Some Mixed Boundary Value Problems"--April 1964.
   Means of applying known displacements and known stresses to the boundaries of models used in experimental stress analysis are given. The application of some of these methods to the analysis of stresses in the field of solid propellant grains is illustrated. The presence of the "pinching effect" is discussed.

5. A. J. Durelli, "Brief Review of the State of the Art and Expected Advance in Experimental Stress and Strain Analysis of Solid Propellant Grains"--April 1964.
   A brief review is made of the state of the experimental stress and strain analysis of solid propellant grains. A discussion of the prospects for the next fifteen years is added.

6. A. J. Durelli, "Experimental Strain and Stress Analysis of Solid Propellant Rocket Motors"--March 1965.
   A review is made of the experimental methods used to strain-analyze solid propellant rocket motor shells and grains when subjected to different loading conditions. Methods directed at the determination of strains in actual rockets are included.

7. L. Ferrer, V. J. Parks and A. J. Durelli, "An Experimental Method to Analyze Gravitational Stresses in Two-Dimensional Problems"--October 1965.
   Photoelasticity and moiré methods are used to solve two-dimensional problems in which gravity-stresses are present.

8. A. J. Durelli, V. J. Parks and C. J. del Rio, "Stresses in a Square Slab Bonded on One Face to a Rigid Plate and Shrunk"--November 1965.
A square epoxy slab was bonded to a rigid plate on one of its faces in the process of curing. In the same process the photoelastic effects associated with a state of restrained shrinkage were "frozen-in." Three-dimensional photoelasticity was used in the analysis.

9. A. J. Durelli, V. J. Parks and C. J. del Rio, "Experimental Determination of Stresses and Displacements in Thick-Wall Cylinders of Complicated Shape"--April 1966.
Photoelasticity and moiré are used to analyze a three-dimensional rocket shape with a star shaped core subjected to internal pressure.

10. V. J. Parks, A. J. Durelli and L. Ferrer, "Gravitational Stresses Determined Using Immersion Techniques"--July 1966.
The methods presented in Technical Report No. 7 above are extended to three-dimensions. Immersion is used to increase response.

11. A. J. Durelli and V. J. Parks. "Experimental Stress Analysis of Loaded Boundaries in Two-Dimensional Second Boundary Value Problems"--February 1967.
The pinching effect that occurs in two-dimensional bonding problems, noted in Reports 2 and 4 above, is analyzed in some detail.

12. A. J. Durelli, V. J. Parks, H. C. Feng and F. Chiang, "Strains and Stresses in Matrices with Inserts,"-- May 1967.
Stresses and strains along the interfaces, and near the fiber ends, for different fiber end configurations, are studied in detail.

13. A. J. Durelli, V. J. Parks and S. Uribe, "Optimization of a Slot End Configuration in a Finite Plate Subjected to Uniformly Distributed Load,"--June 1967.
Two-dimensional photoelasticity was used to study various elliptical ends to a slot, and determine which would give the lowest stress concentration for a load normal to the slot length.

14. A. J. Durelli, V. J. Parks and Han-Chow Lee, "Stresses in a Split Cylinder Bonded to a Case and Subjected to Restrained Shrinkage,"--January 1968.
A three-dimensional photoelastic study that describes a method and shows results for the stresses on the free boundaries and at the bonded interface of a solid propellant rocket.

15. A. J. Durelli, "Experimental Stress Analysis Activities in Selected European Laboratories"--August 1968.
This report has been written following a trip conducted by the author through several European countries. A list is given of many of the laboratories doing important experimental stress analysis work and of the people interested in this kind of work. An attempt has been made to abstract the main characteristics of the methods used in some of the countries visited.

16. V. J. Parks, A. J. Durelli and L. Ferrer, "Constant Acceleration Stresses in a Composite Body"--October 1968.
Use of the immersion analogy to determine gravitational stresses in two-dimensional bodies made of materials with different properties.

17. A. J. Durelli, J. A. Clark and A. Kochev, "Experimental Analysis of High Frequency Stress Waves in a Ring"--October 1968.
A method for the complete experimental determination of dynamic stress distributions in a ring is demonstrated. Photoelastic data is supplemented by measurements with a capacitance gage used as a dynamic lateral extensometer.

18. J. A. Clark and A. J. Durelli, "A Modified Method of Holographic Interferometry for Static and Dynamic Photoelasticity"--April 1968.
A simplified absolute retardation approach to photoelastic analysis is described. Dynamic isopachics are presented.

19. J. A. Clark and A. J. Durelli, "Photoelastic Analysis of Flexural Waves in a Bar"--May 1969.
A complete direct, full-field optical determination of dynamic stress distribution is illustrated. The method is applied to the study of flexural waves propagating in a urethane rubber bar. Results are compared with approximate theories of flexural waves.

20. J. A. Clark and A. J. Durelli, "Optical Analysis of Vibrations in Continuous Media"--June 1969.
Optical methods of vibration analysis are described which are independent of assumptions associated with theories of wave propagation. Methods are illustrated with studies of transverse waves in prestressed bars, snap loading of bars and motion of a fluid surrounding a vibrating bar.

21. V. J. Parks, A. J. Durelli, K. Chandrashekhara and T. L. Chen, "Stress Distribution Around a Circular Bar, with Flat and Spherical Ends, Embedded in a Matrix in a Triaxial Stress Field"--July 1969.
A Three-dimensional photoelastic method to determine stresses in composite materials is applied to this basic shape. The analyses of models with different loads are combined to obtain stresses for the triaxial cases.

22. A. J. Durelli, V. J. Parks and L. Ferrer, "Stresses in Solid and Hollow Spheres Subjected to Gravity or to Normal Surface Tractions"--October 1969.
The method described in Report No. 10 above is applied to two specific problems. An approach is suggested to extend the solutions to a class of surface traction problems.

23. J. A. Clark and A. J. Durelli, "Separation of Additive and Subtractive Moiré Patterns"--December 1969.
A spatial filtering technique for adding and subtracting images of several gratings is described and employed to determine the whole field of Cartesian shears and rigid rotations.

24. R. J. Sanford and A. J. Durelli, "Interpretation of Fringes in Stress-Holo-Interferometry"--July 1970.
Errors associated with interpreting stress-holo-interferometry patterns as the superposition of isopachics (with half order fringe shifts) and isochromatics are analyzed theoretically and illustrated with computer generated holographic interference patterns.

25. J. A. Clark, A. J. Durelli and P. A. Laura, "On the Effect of Initial Stress on the Propagation of Flexural Waves in Elastic Rectangular Bars"--December 1970.
Experimental analysis of the propagation of flexural waves in prismatic, elastic bars with and without prestressing. The effects of prestressing by axial tension, axial compression and pure bending are illustrated.

26. A. J. Durelli and J. A. Clark, "Experimental Analysis of Stresses in a Buoy-Cable System Using a Birefringent Fluid"--February 1971.
An extension of the method of photoviscous analysis is presented which permits quantitative studies of strains associated with steady state vibrations of immersed structures. The method is applied in an investigation of one form of behavior of buoy-cable systems loaded by the action of surface waves.

27. A. J. Durelli and T. L. Chen, "Displacements and Finite-Strain Fields in a Sphere Subjected to Large Deformations"--February 1972.
Displacements and strains (ranging from 0.001 to 0.50) are determined in a polyurethane sphere subjected to several levels of diametral compression. A 500 lines-per-inch grating was embedded in a meridian plane of the sphere and moiré effect produced with a non-deformed master. The maximum applied vertical displacement reduced the diameter of the sphere by 27 per cent.

28. A. J. Durelli and S. Machida, "Stresses and Strain in a Disk with Variable Modulus of Elasticity"--March 1972.
A transparent material with variable modulus of elasticity has been manufactured that exhibits good photoelastic properties and can also be strain analyzed by moiré. The results obtained suggests that the stress distribution in the homogeneous disk. It also indicates that the strain fields in both cases are very different, but that it is possible, approximately, to obtain the stress field from the strain field using the value of E at every point, and Hooke's law.

29. A. J. Durelli and J. Buitrago, "State of Stress and Strain in A Rectangular Belt Pulled Over a Cylindrical Pulley"--June 1972.
Two- and three-dimensional photoelasticity as well as electrical strain gages, dial gages and micrometers are used to determine the stress distribution in a belt-pulley system. Contact and tangential stress for various contact angles and friction coefficients are given.

30. T. L. Chen and A. J. Durelli, "Stress Field in a Sphere Subjected to Large Deformations"--June 1972.
Strain fields obtained in a sphere subjected to large diametral compressions from a previous paper were converted into stress fields using two approaches. First, the concept of strain-energy function for an isotropic elastic body was used. Then the stress field was determined with the Hookean type natural stress-natural strain relation. The results so obtained were also compared.

31. A. J. Durelli, V. J. Parks and H. M. Hasseem, "Helices Under Load"--July 1973.
Previous solutions for the case of close coiled helical springs and for helices made of thin bars are extended. The complete solution is presented in graphs for the use of designers. The theoretical development is correlated with experiments.

32. T. L. Chen and A. J. Durelli, "Displacements and Finite Strain Fields in a Hollow Sphere Subjected to Large Elastic Deformations"--September 1973.
The same methods described in No. 27, were applied to a hollow sphere with an inner diameter one half the outer diameter. The hollow sphere was loaded up to a strain of 30 per cent on the meridian plane and a reduction of the diameter by 20 per cent.

33. A. J. Durelli, H. H. Hasseem and V. J. Parks, "New Experimental Method in Three-Dimensional Elastostatics"--December 1973.
A new material is reported which is unique among three-dimensional stress-freezing materials, in that, in its heated (or rubbery) state it has a Poisson's ratio which is appreciably lower than 0.5. For a loaded model, made of this material, the unique property allows the direct determination of stresses from strain measurements taken at interior points in the model.

34. J. Wolak and V. J. Parks, "Evaluation of Large Strains in Industrial Applications"--April 1974.
It was shown that Mohr's circle permits the transformation of strain from one axis of reference to another, irrespective of the magnitude of the strain, and leads to the evaluation of the principal strain components from the measurement of direct strain in three directions.

35. A. J. Durelli, "Experimental Stress Analysis Activities in Selected European Laboratories"--April 1975.
Continuation of Report No. 15 after a visit to Belgium, Holland, Germany, France, Turkey, England and Scotland.

36. A. J. Durelli, V. J. Parks and J. O. Bühler-Vidal, "Linear and Non-linear Elastic and Plastic Strains in a Plate with a Big Hole Loaded Axially in its Plane"--July 1975.
Strain analysis of the ligament of a plate with a big hole indicates that both geometric and material non-linearity may take place. The strain concentration factor was found to vary from 1 to 2 depending on the level of deformation.

37. A. J. Durelli, V. Pavlin, J. O. Bühler-Vidal and G. Ome, "Elastostatics of a Cubic Box Subjected to Concentrated Loads"--August 1975.
Analysis of experimental strain, stress and deflection of a cubic box subjected to concentrated loads applied at the center of two opposite faces. The ratio between the inside span and the wall thickness was varied between approximately 5 and 121.

38. A. J. Durelli, V. J. Parks and J. O. Bühler-Vidal, "Elastostatics of Cubic Boxes Subjected to Pressure"--March 1976.
Experimental analysis of strain, stress and deflections in a cubic box subjected to either internal or external pressure. Inside span-to-wall thickness ratio varied from 5 to 14.

39. Y. Y. Hung, J. D. Hovanesian and A. J. Durelli, "New Optical Method to Determine Vibration-Induced Strains with Variable Sensitivity After Recording"--November 1976.
A steady state vibrating object is illuminated with coherent light and its image slightly misfocused. The resulting specklegram is "time-integrated" as when Fourier filtered gives derivatives of the vibrational amplitude.

40. Y. Y. Hung, C. Y. Liang, J. D. Hovanesian and A. J. Durelli, "Cyclic Stress Studies by Time-Averaged Photoelasticity"--November 1976.
"Time-averaged isochromatics" are formed when the photographic film is exposed for more than one period. Fringes represent amplitudes of the oscillating stress according to the zeroth order Bessel function.

41. Y. Y. Hung, C. Y. Liang, J. D. Hovanesian and A. J. Durelli, "Time-Averaged Shadow Moiré Method for Studying Vibrations"--November 1976.
Time-averaged shadow moiré permits the determination of the amplitude distribution of the deflection of a steady vibrating plate.

42. J. Buitrago and A. J. Durelli, "On the Interpretation of Shadow-Moiré Fringes"--April 1977.
Possible rotations and translations of the grating are considered in a general expression to interpret shadow-moiré fringes and on the sensitivity of the method. Application to an inverted perforted tube.

43. J. der Hovanesian, "18th Polish Solid Mechanics Conference." Published in European Scientific Notes of the Office of Naval Research, in London, England, Dec. 31, 1976.
Comments on the planning and organization of, and scientific content of paper presented at the 18th Polish Solid Mechanics Conference held in Wisla-Jawornik from September 7-14, 1976.

44. A. J. Durelli, "The Difficult Choice," -- May 1977.
The advantages and limitations of methods available for the analyses of displacements, strain, and stresses are considered. Comments are made on several theoretical approaches, in particular approximate methods, and attention is concentrated on experimental methods: photoelasticity, moiré, brittle and photoelastic coatings, gages, grids, holography and speckle to solve two- and three-dimensional problems in elasticity, plasticity, dynamics and anisotropy.

45. C. Y. Liang, Y. Y. Hung, A. J. Durelli and J. D. Hovanesian, "Direct Determination of Flexural Strains in Plates Using Projected Gratings," -- June 1977
The method requires the rotation of one photograph of the deformed grating over a copy of itself. The moiré produced yields strains by optical double differentiation of deflections. Applied to projected gratings the idea permits the study of plates subjected to much larger deflections than the ones that can be studied with holograms.

OPTIMIZATION OF GEOMETRIC DISCONTINUITIES IN STRESS FIELDS

Introduction

Some fifty years ago the subject of stress concentrations deserved a great deal of interest from scientists and engineers. Changes in the uniform shape of a component disturb the stress distribution, and most of the time increases the maximum stress. This fact was likely to have an influence on failure and excited the imagination of theoreticians first, and experimentalists later, to find means to determine the value of the increase in stress. Kirsch[1] was probably the first one who obtained a meaningful answer to the problem when he presented the equations giving the stress distribution around an empty circular hole. Today, several handbooks summarize the findings on stress concentrations and make them available to engineers in an easy-to-use form. Among the most popular, the books by Peterson[2] and Roark[3] can be mentioned.

Scientists and engineers, after worrying about the increase in stress associated with changes in shape, are beginning to consider now the possibility of controlling those changes to minimize the stress and optimize the shape. It seems logical in the development of these studies that the optimization of shapes has to follow the knowledge of the stress concentrations. The subject is of particular importance today when mankind will be making a strong effort to save energy and materials. The methods and criteria to be presented in this paper are general, but the new examples of application have been selected less for the technological importance than as illustrations and means of exciting the imagination of designers and students.

Previous Contributions

Optimization of the shape of fillets and holes in stress fields has interested few people so far. One of the first references, by implication, can be found in a discussion by Richmond[4] of a paper by Mindlin. It is pointed out that if a square tunnel with rounded corners is present in a semi-space, there is a particular value of the radius of the fillets at the corners of the square that will optimize the stress distribution. Whether the value of the radius is smaller or larger than $\frac{D}{6}$, D being the side of the square, the stress concentration will increase.

An important contribution was made in an early paper by Berkey[5] who studied systematically the stress concentration associated with elliptical fillets with the purpose of reducing the concentration at a shoulder. The attempts by Baud[6] and by Lansard[7] should be mentioned in spite of the unfortunate reference to a non-existing analogy. Some further reference to the problem is implied in a section in Peterson's handbook[8] when the study of concentrations associated with noncircular fillets is introduced.

Kuske[9] refers to the problem but it is in Heywood's[10][11] books where the subject has been dealt with more extensively, and in a more practical way.

Sometime ago the author used the concept of an ideal fillet, defined it as a fillet without stress concentration and related it photoelastically to the coincidence of the boundary with an isochromatic fringe. Some references can be found in a book[12], reports and early papers[13][14][15]. Recently Francavilla et al[16] attempted the optimization of fillets using finite element methods. The geometries they obtained,however,show some stress concentration. In this paper, besides reviewing the problem of the

optimization of holes and fillets, the concept of efficiency factor will be introduced, and attempts will be made at optimizing complete boundaries, even those subjected to stresses of opposite signs.

For the purpose of completeness it should be mentioned that another approach has been followed sometimes, with the same objective of increasing strength by decreasing weight. It consists in adding new discontinuities to the original one. So it can be shown that a row of holes, or fillets may produce a smaller stress concentration than a single hole, or fillet. One of the first contributions to this method was made by Thum and Svenson [17]. Further studies can be found in other papers by one of the authors [18][19] and more recently by Erickson and Riley [20]. The scope of this paper is limited to the optimization by changing the contour of the discontinuity.

Approach to the Solution

It is possible to use a computer and an appropriate program to develop a contour that will minimize the stress as was done in [16]. It seems more efficient, however, to use photoelasticity. Two-dimensional photoelasticity is very well developed by now, and the machining of models and the photographing of records can be done as routine operations in well-organized laboratories. The optimization can be accomplished by manual filing of boundaries as suggested in (12).

The proposed method has already been applied to the solution of two problems of technological interest: 1) the tip of the several rays of stars in perforated solid propellant grains used for rocket propulsion, and 2) the transition between the blade and the dove-tail joint in a turbine.

The tip of the star in solid propellant grains was originally designed either with one circular fillet tangent to the two sides of each ray or with

a flat botton connected through two small circular fillets to the sides of each ray (Fig. 1). In the first case the maximum stress, given in a photoelastic model by the maximum order of the isochromatic fringe, is at the axis of the ray. In the second case, left side of Fig. 1, the maximum stress takes place at the corners. It can be observed that at these points both the fringe order and the density of the fringes are higher. A very small amount of material at the boundary of the fillet is subjected to a very high stress.

The second example refers to the transition between the blade and the dove-tail that joins it to the rotor of the turbine. It was originally designed using circular fillets, of relatively large radii in this case, as shown on the left of Fig. 2. The isochromatic pattern in the photoelastic model indicates dense fringes with a high order at the bottom of the fillet.

The appearance of isochromatic fringes at the boundary of ideal fillets is shown on the right side of Figs. 1 and 2. The deciding characteristic is that a fringe coincides with appreciable length of the boundary of the fillet. When the boundary intersects another fringe the latter is of a lower order. Strain, and energy, therefore are not concentrated on a small portion of the boundary but distributed on a long part of it. An even more striking example is shown in Fig. 3 which represents the tip of a star in a solid propellant grain.

The transformation of the shape from the original design to the optimum design shown on the right side of the figures can be done in a relatively short time with a hand file. The operator starts removing material by filing off zones of low stress. This decreases the order of the fringe at the zone of concentration and increases it at the zone of low stress. If the

operation is conducted in a large field diffused light polariscope the operator can watch the transferring of fringes as he files and in a short while reaches the moment when one single fringe coincides with the boundary of the model. The manual operation of filing may introduce some logical irregularities as shown in Fig. 1. If more precision is desired a second model should be machined as shown in Fig. 2, with a fillet shape corresponding to the one obtained by filing and, if necessary, further refinement can be obtained by applying the same operation of filing to the second model. In the two cases reported above the optimum shape is obtained after only slight changes in geometry.

From a practical point-of-view a further consideration should be made. It has been found that frequently the optimum fillet shape can be fitted with two or more circles so that neighboring circles have common tangents.

Criteria

The definition of the problem requires the specification of the constraints imposed by the design. In the two cases mentioned above the optimization was obtained with very little change in geometry. That was all that was permitted by the functional requirements. Of course, the optimization problem may have several answers if the functional requirements permit appreciable changes in design.

An improved design, obtained following the procedure outlined above, always brings the stress concentration value down. However, it may not always be clear whether the design is optimum. It is proposed here that the "degree of optimization" be evaluated quantitatively as a coefficient of efficiency, k_{eff}. For the case where the tangential stress σ_t is of

the same sign all along the boundary, k_{eff} can be defined as

$$k_{eff} = \int_{S_0}^{S_1} \frac{\sigma_t ds}{(S_1 - S_0)\sigma_{all}}$$

where σ_{all} represents the maximum allowable stress and S_1 and S_0 are the limiting points along the boundary. For the case of both tensile and compressive stresses, k_{eff} is computed as a weighted average of the efficiency factors along the tensile and compressive portions of the boundary. Taking the weighting factor in terms of boundary lengths yields

$$k_{eff} = \frac{\int_{S_0}^{S_1} \sigma_t^+ ds}{(S_1 - S_0)\sigma_{all}^+} \frac{S_1 - S_0}{S_2 - S_0} + \frac{\int_{S_1}^{S_2} \sigma_t^- ds}{(S_2 - S_1)\sigma_{all}^-} \frac{S_2 - S_1}{S_2 - S_0}$$

$$k_{eff} = \frac{1}{S_2 - S_0} \left\{ \frac{\int_{S_0}^{S_1} \sigma_t^+ ds}{\sigma_{all}^+} + \frac{\int_{S_1}^{S_2} \sigma_t^- ds}{\sigma_{all}^-} \right\}$$

where the positive and negative superscripts refer to tensile and compressive stresses respectively.

A coefficient of efficiency equal to one is a limiting case and corresponds to a boundary without stress concentration, subjected everywhere to the same stress. The circular hole in a hydrostatic field is an example. The closer k_{eff} is to one, the more efficient the design.

The criteria for optimization will depend on the criterion for failure. If the boundary to be optimized is subjected to both positive and negative stresses, the integration along the boundary should be conducted using absolute values for the stresses. If the component is designed for a material that has the same allowable maximum stress under tension as under compression, the ideal shape would have equal values for both peak stresses, the tensile and the compressive. If, as is the case for brittle materials, the maximum allowable tensile stress is only a fraction of the maximum allowable compressive stress, the ratio between the two peak stresses in the optimum design would be the same as the ratio of the two allowable maximum stresses.

The redesign of a circular tube or ring, to optimize the inside boundary, will be used as example of the application of the criteria and the procedure mentioned above. The problem has application in the field of tunnel and pipe design, but it will be presented mainly as an academic problem to illustrate the method. It will be assumed that the material to be used in the manufacture of the tube has the same maximum allowable tensile and compressive stresses. Another example to be shown will be the case of a thin straight bar of rectangular cross-section. The bar has a transverse circular hole and is subjected to axial loading. The optimization will be conducted for a different allowable stress in tension and in compression.

The Ring Under Diametral Compression

The circular ring subjected to diametral compression has been the object of many experimental analyses (see among others (21)). In a future paper it is planned to study parametrically the properties of the ring as the ratio between the outside and inside diameters varies and to attempt

optimization of the inside boundary for the whole range of thickness. In this paper the procedure will be illustrated for the case $\frac{ID}{OD} = 0.53$. The constraints of the problem are: a) the outside boundary has to be kept circular; b) the inside boundary has to clear the circle of diameter 0.53 OD; c) the allowable maximum stress for tension is the same as for compression.

Optimization of the Ring

Two stress concentration factors (taking the average σ_y over the horizontal section of symmetry as reference) are of particular interest. The one of compression takes place at the intersection of the inside boundary with the horizontal axis and the one of tension at the intersection of the vertical axis with the same boundary. For the $\frac{ID}{OD} = 0.53$ ring these factors are 6.0 and 6.6 respectively. The efficiency coefficient is 0.587.

Following the procedure of removing material from low stress regions the shape shown in Fig. 4 was developed. Photoelastic analysis of the pattern indicates that both stress concentration factors have decreased to 5 and the efficiency coefficient has increased to 0.952. The tensile stress concentration which is the governing one in many designs has been decreased by nearly 25%. The saving in the weight of the material used is 10%.

The stress distribution over the inside boundary for the circular ring and for the optimized geometry is shown in Fig. 5.

The empirically developed inside geometry has been fitted with a combination of circles of different diameters and common tangents at the points of intersections. The geometry of the optimized shape is shown in Fig. 6.

The improvement obtained in the strength of rings designed using optimized inside boundaries has been determined by breaking three plain circular rings and three optimized rings, made of 0.5 in. thick Homelite 100 plates. The increase in strength was 20.6%. The range of values of each set of measurements was limited by a variation of $\pm$ 6% of the average.

The Perforated Plate Under Axial Loading

In industrial applications a plate may have to be perforated for different reasons: to permit the passage of another component (a bar for instance) or to make the plate lighter, and still sufficiently rigid. In the case of walls, or tunnels, the perforation is a passage. Frequently the geometry given to the perforation is circular, but for functional requirements the perforation may be square, or rectangular.

The maximum stress on the edge of the circular hole takes place at the transverse cross-section and for the very wide plate its order is 3 when the stress on the gross area is taken as reference. A stress of opposite sign, of order 1, on the edge of the hole takes place at the longitudinal axis. As the width of the plated decreases in relation to the diameter of the hole, those values of stresses increase. If material used for the plate is metal, and the plate is subjected to axial tensile loading, points on the edge of the boundary near the transverse cross-section are much closer to failure than those near the longitudinal cross-section (unless buckling is involved). If the problem is a tunnel under compressive load, and the material used is brittle, the points at the longitudinal axis may fail under tension, much before those at the transverse axis would fail under compression. Similar considerations can be applied to the square hole, the situation being more complicated because of the possible appearance of concentrations at the corners.

The optimization of this type of discontinuity depends on the relation between the width W of the plate and the diameter D of the hole, and on the relative allowable stress of the material under tension and compression. The optimization procedure will be illustrated for the case $\frac{D}{W} = 0.6$ The constraints of the problem are: a) the inside boundary has to lie inbetween the circle of diameter D and the square of side D; b) the allowable maximum stress for compression is 2.3 times the allowable stress for tension (case of some brittle materials).

Optimization of the Hole in the Plate

The stress concentration factors (taking the average σ_y over the transverse gross area as reference) are of particular interest. The one at the transverse axis is 5.1 for the circular hole, and 3.77 for the optimized hole; the one at the longitudinal axis is 2.2 for the circular hole and 1.63 for the optimized hole. The maximum stresses have been reduced by 26%. The size of the hole has been increased by 22.8%.

The efficiency coefficient of the circular hole is 54%. The efficiency coefficient of the optimized hole is 90%.

Conclusion

It has been shown that two-dimensional photoelasticity can be used effectively to optimize the boundaries of plates loaded in their plane. The concept of "coefficient of efficiency" has been introduced to evaluate the degree of the optimization. Two illustrative problems have been solved: a circular tube (or ring) under diametral compression and a perforated plate loaded axially. The efficiency coefficient of the tube

has been increased from 0.587 to 0.952, and the one of the plate from 0.54 to 0.90. In both cases the maximum stress has been decreased by about 25%. The weight of the ring has been reduced by 10% and the size of the hole of the plate has been increased by about 23%. The increase in the strength of the ring made of a brittle material was 20.6%.

Acknowledgments

The research program described in this paper has been supported financially in part by the National Science Foundation (Grant ENG77-07974) and in part by the Office of Naval Research (N00014-76-C-0487) and with funds of the John F. Dodge chair at Oakland University. The authors would like to express their appreciation for this support, in particular to C. Astill, monitor of the NSF grant and N. Perrone and N. Basdekas, monitors of the ONR contract. The reproduction of the manuscript was prepared by M. Wood.

REFERENCES

1. Kirsch B., "Theory of Elasticity and Requirements of Strength of Materials,"Zeits, Ver, Deut. Ing. Vol. 42, 1898, p. 799
2. Peterson R. E., "Stress Concentration Factors," Wiley, 1974.
3. Roark R. J. and Young, W. C., "Formulas for Stress and Strain," McGraw-Hill, 1975, Fifth Edition.
4. Richmond W. O., Discussion of R. D. Midlin's paper on "Stress Distribution Around a Tunnel," Proc. ASCE, Oct. 1939, pp. 1465-1467.
5. Berkey D. C., "Reducing Stress Concentration with Elliptical Fillets," Proc. SESA, Vol. 1, No. 2, 1944, pp. 56-60
6. Baud R. V., Beitraege zur Kenntnis der Spannungsverteilung in Prismatischen und Keilfoermigen Konstruktionselementen mit Querschnitteubergaengen.," Eidg., Materialpruef. Ber. Vol. 83, Zuerich 1934.
7. Lansard R., "Fillets without Stress Concentration," Proc. SESA, Vol. XIII, No. 1, pp. 97-104, 1955.
8. Peterson R. E., see (2) p. 83.
9. Kuske, A., "Einfuehrung in die Spannungsoptik. Wiss. Verlag, Stuttgart 1959.
10. Heywood R. B., "Designing by Photoelasticity," Chapman and Hall, 1952.
11. Heywood R. B., "Photoelasticity for Designers," Pergamon 1969, Chap. 11.
12. Durelli A. J. and Riley W. F., "Introduction to Photomechanics," Prentice Hall, 1965, p. 228.
13. Durelli A. J., "Experimental Strain and Stress Analysis of Solid Propellant Rocket Motors," Mech. and Chem. of Solid Propellants, Pergamon, 1967, pp. 381-442.

14. Durelli A. J., Dally J. W. and Riley W. F., "Stress and strength Studies on Turbine Blad Attachments," Proc. SESA, Vol. XVI, No. 1, pp. 171-182, presented Oct. 1957.

15. Durelli A. J., Parks V. J. and Uribe S., "Optimization of a Slot End Configuration in a Finite Plate Subjected to Uniformly Distributed Load," Jour. App. Mech. Vol. 35, No. 2, pp. 403-406, June 1968.

16. Francavilla A., Ramakrishnan C. V. and Zienkiewiez O. C., "Optimization of Shape to Minimize Stress Concentration," Jour. Strain An. Vol. 10, No. 2, pp. 63-70, 1976.

17. Thum A. and Svenson O., "Beanspruchung bei mehrfacher Kerkwirkung. Entlastung-und Ueberlastungskerben," Schweizer Archiv fur Ang. Wiss und Tech. 15th year, Nr. 6, June 1949, pp. 161-174.

18. Durelli A. J., Lake R. L. and Phillips E., "Stress Concentrations Produces by Multiple Semi-circular Notches in Infinite Plates under Uniaxial State of Stress," Proc. SESA, Vol. X, No. 1, pp. 53-64, 1952.

19. Durelli A. J., Lake R. L. and Phillips E., "Stress Distribution in Plates under a Uniaxial State of Stress, with Multiple Semi-circular and Flat-bottom Notches," Proc. First U.S. Nat. Congr. App. Mech, pp. 309-315, 1952.

20. Erickson P. E. and Riley W. F., "Minimizing Stress Concentrations Around Circular Holes in Uniaxially Loaded Plates", presented at S.E.S.A. meeting in Houston, Texas, May, 1977.

21. Durelli A. J. and Parks V. J., "Moiré Analysis of Strain", Prentice Hall, 1970.

BOTTOM OF THE RAYS OF THE STAR-SHAPED CONFIGURATION
OF THE PROPELLANT GRAIN OF A MISSILE

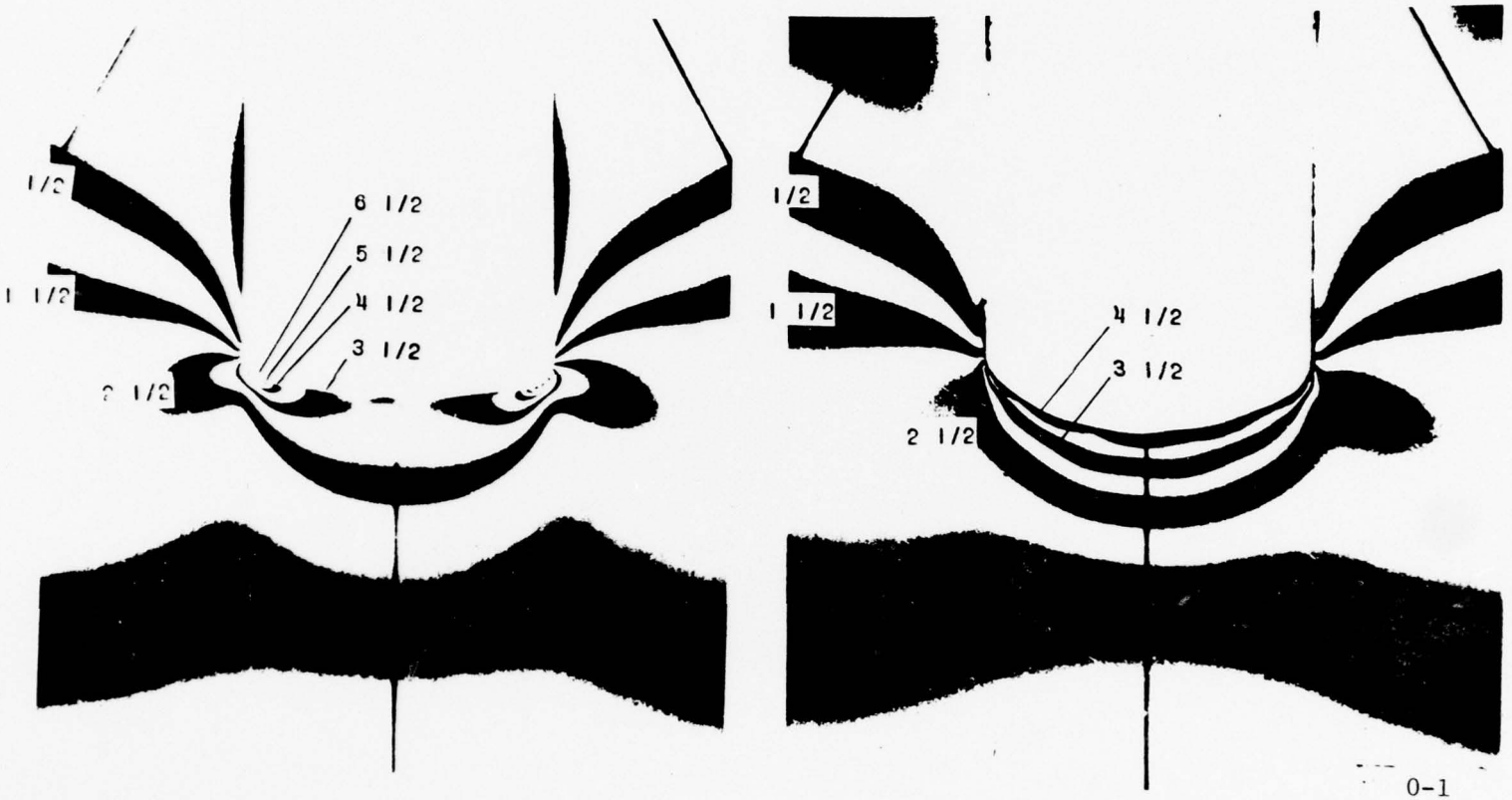

FIG. 1. ISOCHROMATICS OBTAINED FOR THE ORIGINAL AND OPTIMIZED DESIGNS OF A FILLET CONTOUR (When an isochromatic lies along the length of a fillet, the fillet geometry is optimum.)

FILLET AT THE DOVE-TAIL JOINT BETWEEN BLADES AND ROTOR IN A JET ENGINE

Poor Fillet

Ideal Fillet

FIG. 2. ISOCHROMATICS ABOUT A POORLY DESIGNED FILLET AND A NEARLY IDEAL FILLET

BOTTOM OF THE RAYS OF THE STAR-SHAPED CONFIGURATION OF THE PROPELLANT GRAIN OF A MISSILE

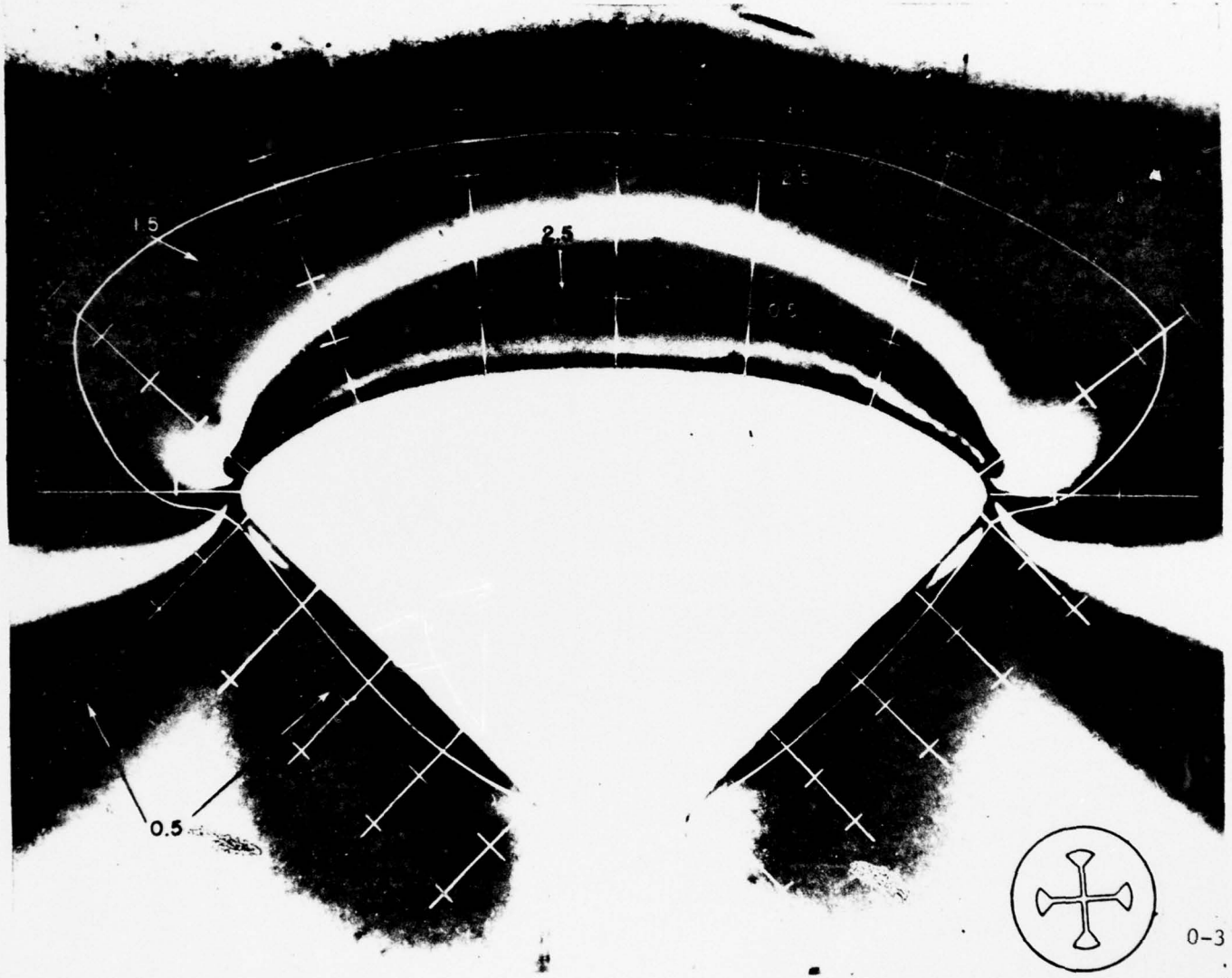

FIG. 3 EXAMPLE OF FILLET OF OPTIMUM SHAPE. THE MAGNITUED OF THE BOUNDARY STRESS IS PROPORTIONAL TO THE DISTANCE BETWEEN THE BOUNDARY AND THE WHITE LINE

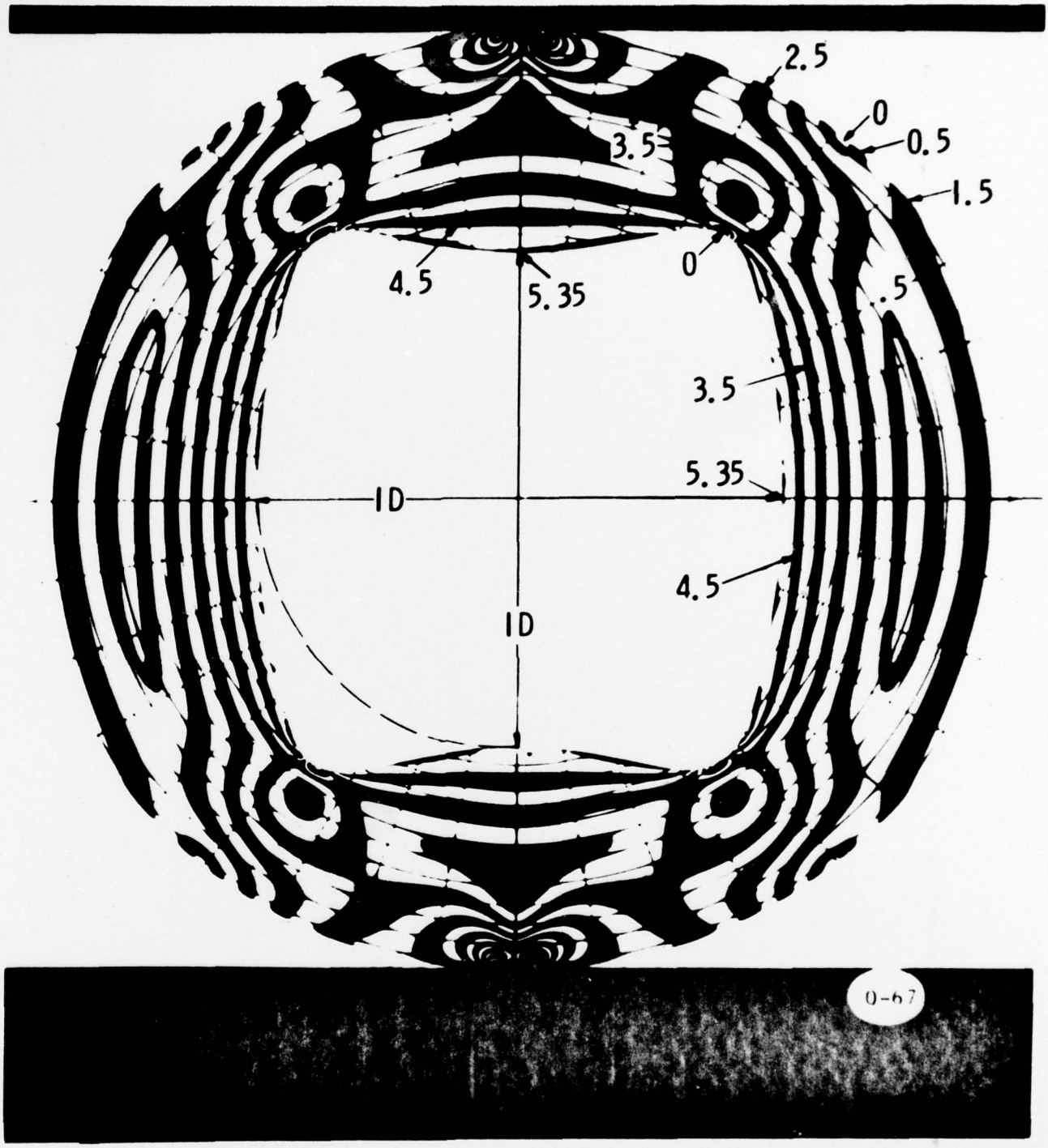

FIG. 4 OPTIMIZATION OF THE INSIDE BOUNDARY OF A CIRCULAR RING SUBJECTED TO DIAMETRAL COMPRESSION

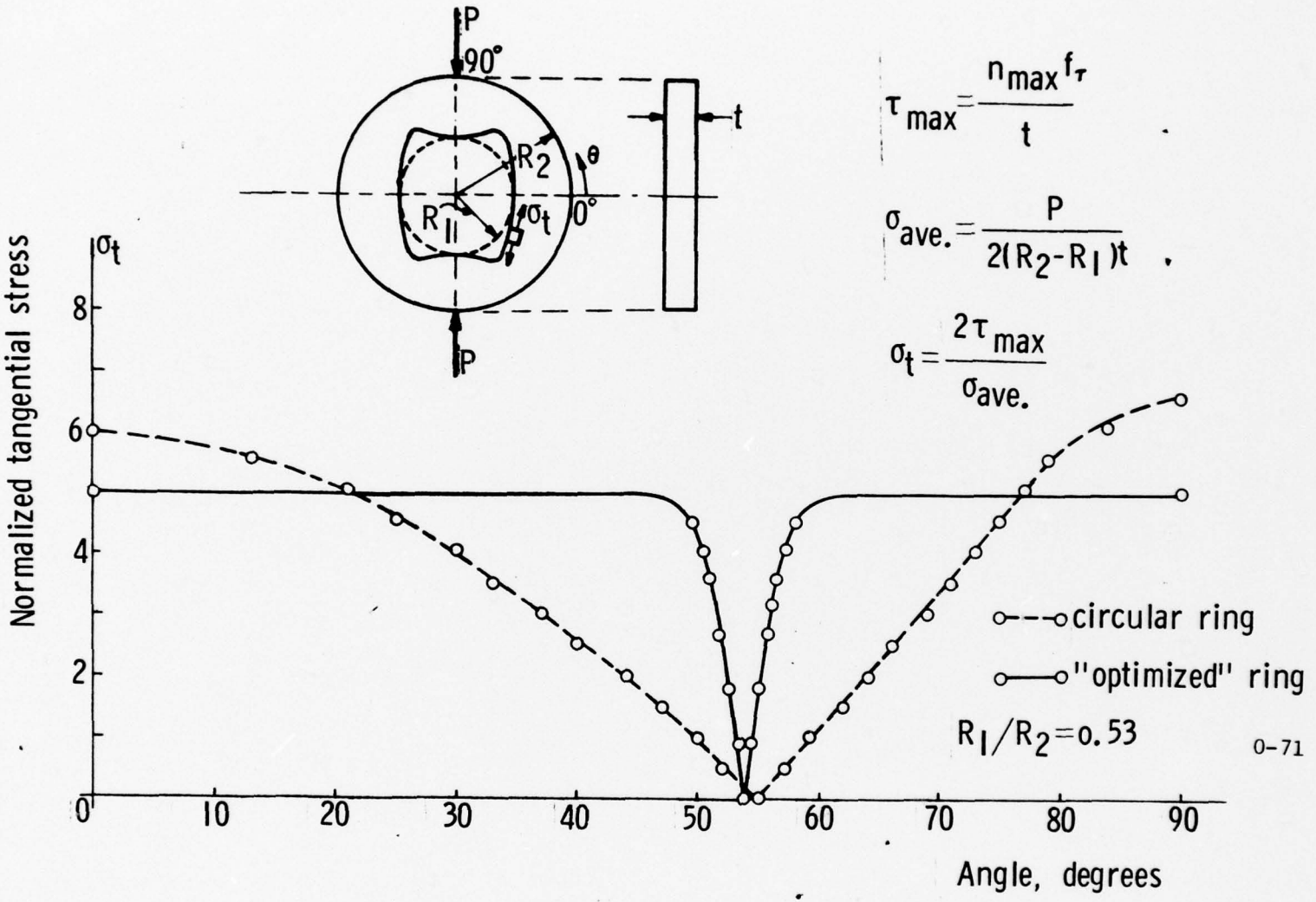

FIG. 5 STRESS TANGENTIAL TO THE BOUNDARY OF AN OPTIMIZED RING SUBJECTED TO DIAMETRICAL COMPRESSION

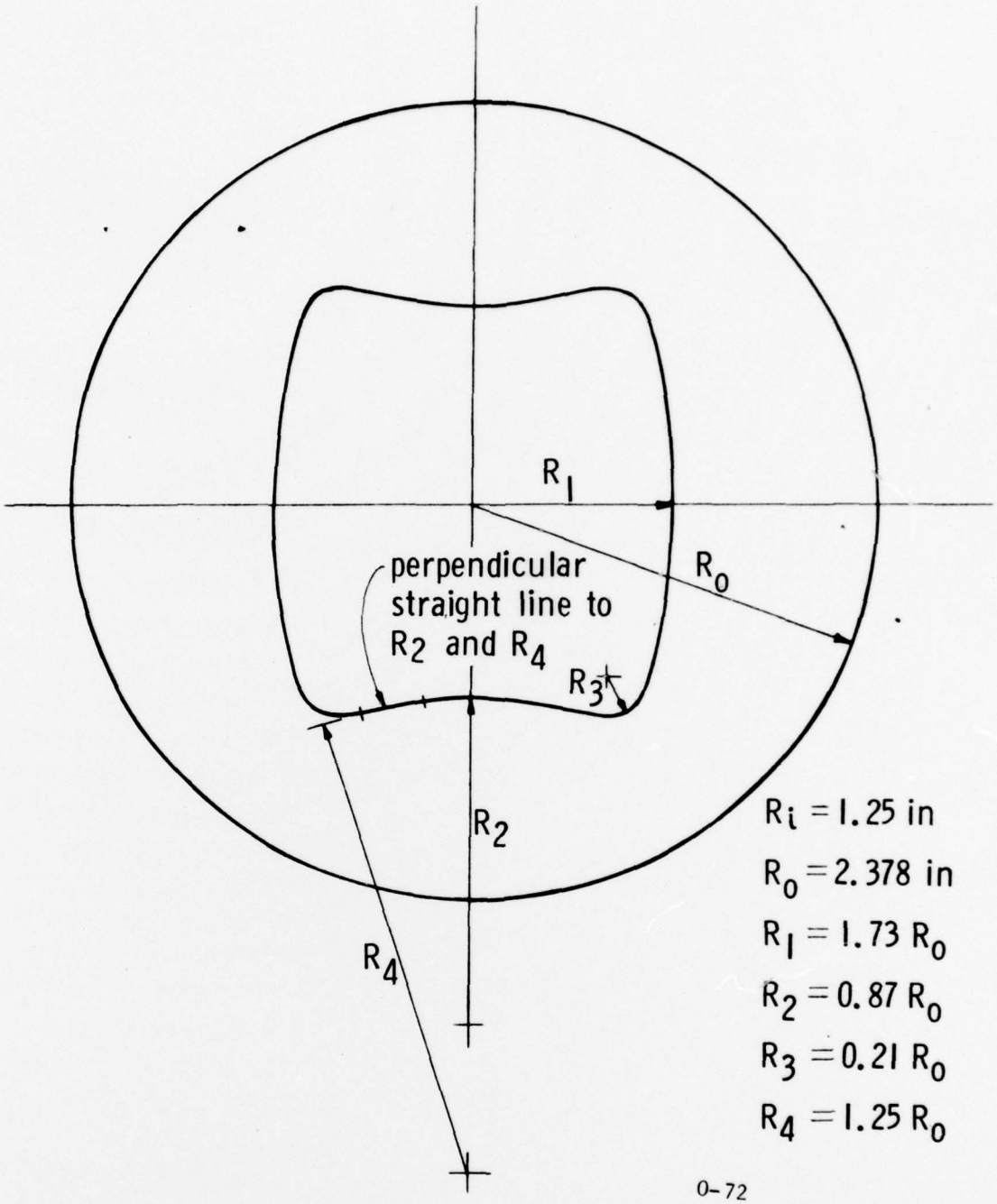

FIG. 6 NON-DIMENSIONALIZED GEOMETRY OF THE OPTIMIZED RING FOR $\frac{ID}{OD} = 0.53$

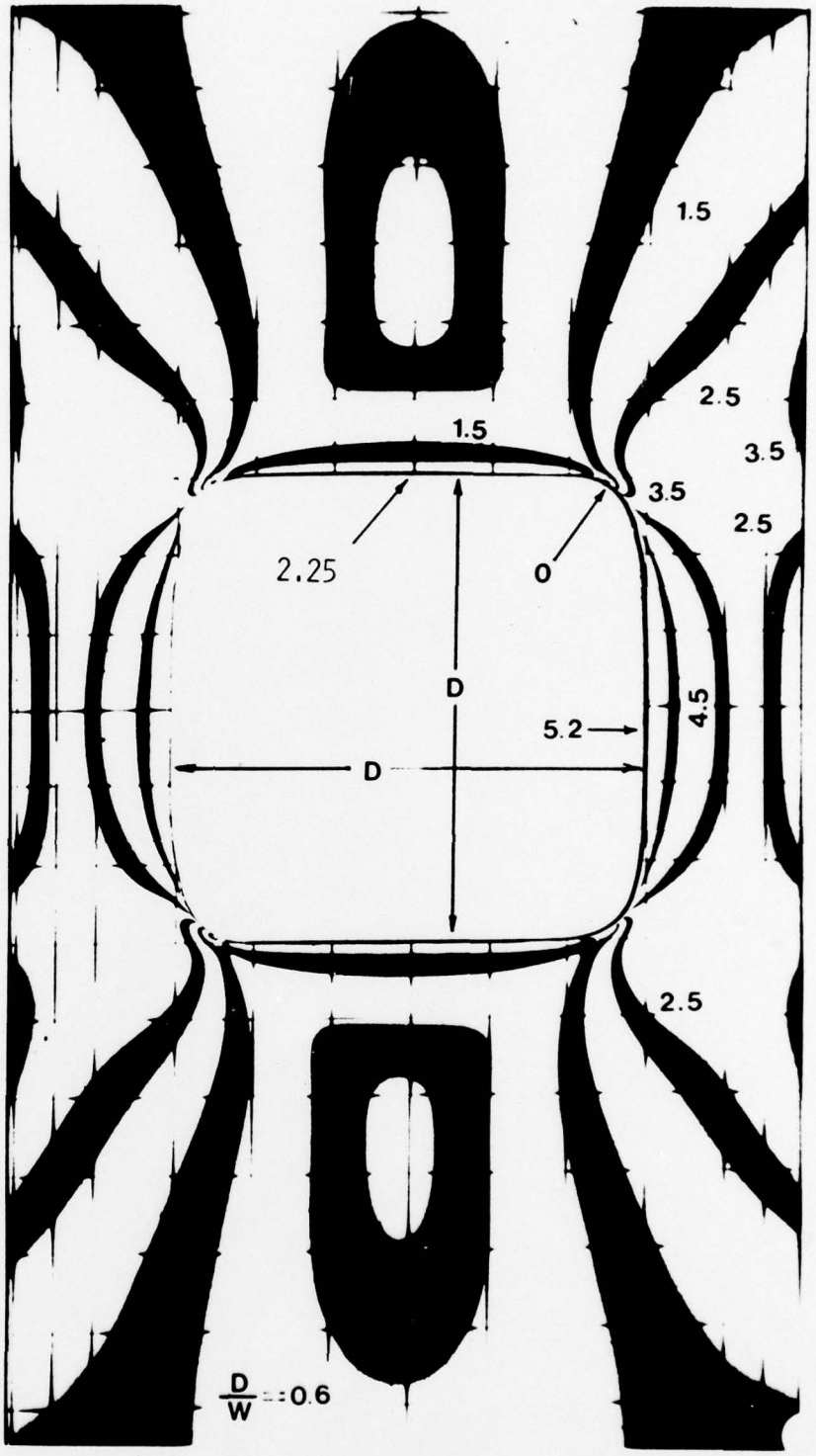

FIG. 7 OPTIMIZATION OF THE BOUNDARY OF A HOLE IN A RECTANGULAR PLATE OF FINITE WIDTH SUBJECTED TO AXIAL LOAD

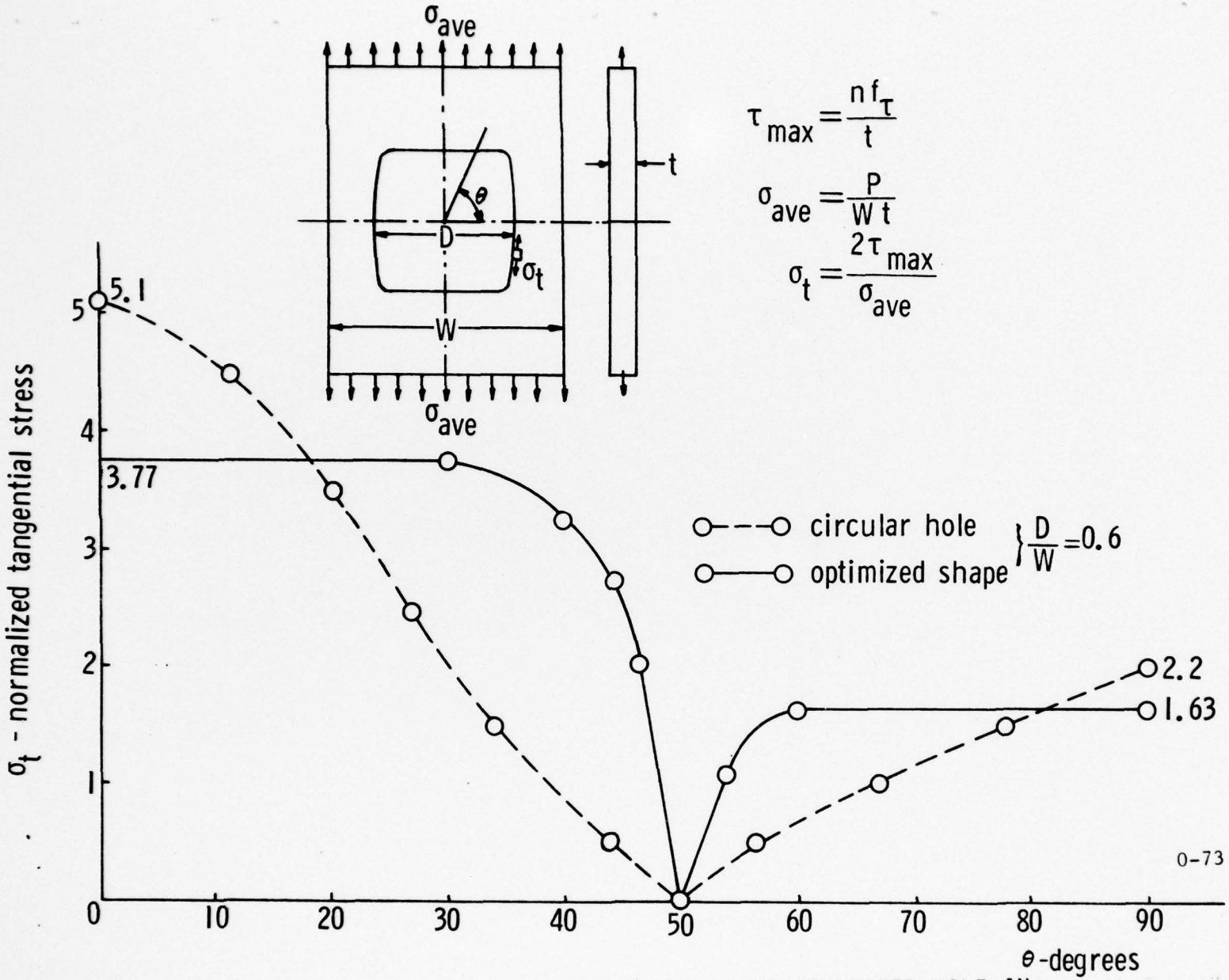

FIG. 8 STRESS TANGENTIAL TO THE BOUNDARY OF AN OPTIMIZED HOLE IN A PLATE SUBJECTED TO AXIAL LOADING ($\frac{D}{W} = 0.6$)

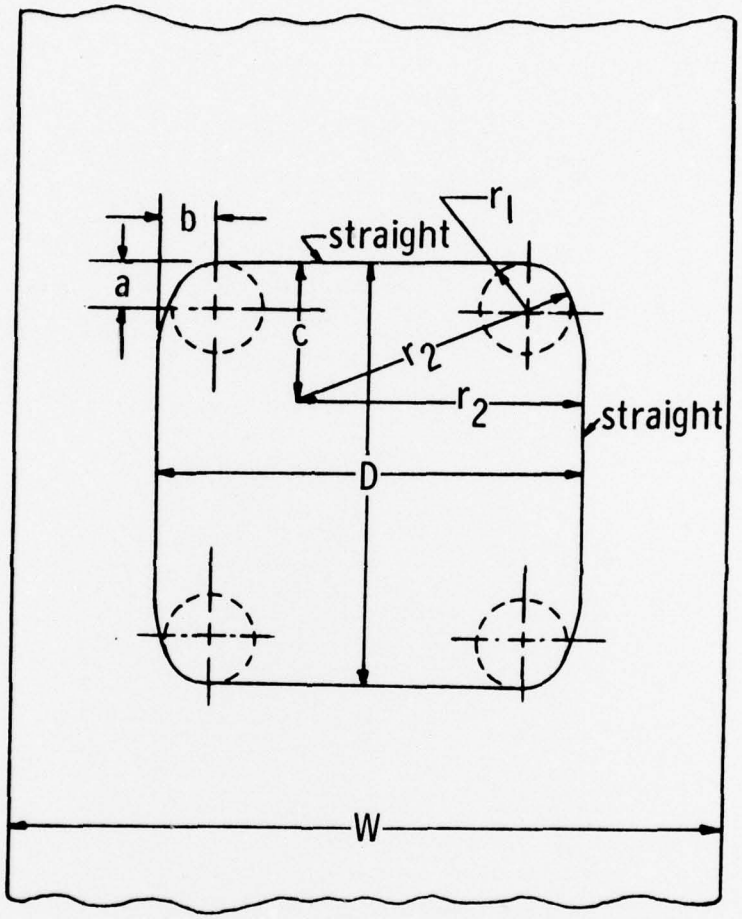

$D = 0.6\,W$

$r_1 = 0.062\,W$

$r_2 = 0.4\,W$

$a = 0.0625\,W$

$b = 0.0875\,W$

$c = 0.19\,W$

0-74

FIG. 9 NON-DIMENSIONALIZED GEOMETRY OF THE OPTIMIZED HOLE IN A PLATE SUBJECTED TO AXIAL LOADING ($\frac{D}{W} = 0.6$)

ONR DISTRIBUTION LIST

Part I - Government

Chief of Naval Research
Department of the Navy
Arlington, Virginia 22217
Attn: Code 474 (2)
471
222

Director
ONR Branch Office
495 Summer Street
Boston, Massachusetts 02210

Director
ONR Branch Office
536 S. Clark Street
Chicago, Illinois 60604

Director
Naval Research Laboratory
Attn: Code 2629 (ONRL)
Washington, D.C. 20390 (6)

U.S. Naval Research Laboratory
Attn: Code 2627
Washington, D.C. 20390

Commanding Officer
ONR Branch Office
207 West 24th Street
New York, N.Y. 10011

Director
ONR Branch Office
1030 E. Green Street
Pasadena, California 91101

Defense Documentation Center
Cameron Station
Alexandria, Virginia 22314 (12)

Army

Commanding Officer
U.S. Army Research Off. Durham
Attn: Mr. J. J. Murray
CRD-AA-IP
Box CM, Duke Station
Durham, North Carolina 27706

Commanding Officer
AMXMR-ATL
Attn: Mr. R. Shea
U.S. Army Materials Res. Agency
Watertown, Massachusetts 02172

Watervliet Arsenal
MAGGS Research Center
Watervliet, New York 12189
Attn: Director of Research

Redstone Scientific Info. Center
Chief, Document Section
U.S. Army Missile Command
Redstone Arsenal, Alabama 35809

Army R &D Center
Fort Belvoir, Virginia 22060

Navy

Commanding Officer & Director
Naval Ship Res. & Dev. Center
Bethesda, Maryland 20034
Attn: Code 042 (Tech. Lib. Br.)
17 (Struc. Mech. Lab.)
172
172
174
177
1800(Appl. Math. Lab.)
5412S (Dr. W.D. Sette)
19 (Dr. M.M. Sevik)
1901 (Dr. M. Strassberg)
1945
196 (Dr. D. Feit)
1962

Naval Weapons Laboratory
Dahlgren, Virginia 22448

Naval Research Laboratory
Washington, D.C. 203
Attn: Code 8400
8410
8430
8440
6300
6390
6380

Undersea Explosion Res. Div.
Naval Ship R&D Center
Norfolk Naval Shipyard
Portsmouth, Virginia 23709
Attn: Dr. E. Palmer
Code 780

Naval Ship Res. & Dev. Center
Annapolis Division
Annapolis, Maryland 21402
Attn: Code 2740 - Dr. Y. F. Wang
28 - Mr. R.J. Wolfe
281 - Mr. Niederberger
2814 - Dr. H. Vanderveldt

Technical Library
Naval Underwater Weapons Center
Pasadena Annex
3202 E. Foothill Blvd.
Pasadena, California 91107

U.S. Naval Weapons Center
China Lake, California 93557
Attn: Code 4062 - Mr. W. Werback
4520 - Mr. Ken Bischel

Commanding Officer
U.S. Naval Civil Engr. Lab.
Code L31
Port Hueneme, California 93041

Technical Director
U.S. Naval Ordnance Lab.
White Oak
Silver Spring, Maryland 20910

Technical Director
Naval Undersea R&D Center
San Diego, California 92132

Supervisor of Shipbuilding
U.S. Navy
Newport News, Virginia 23607

Technanical Director
Mare Island Naval Shipyard
Vallejo, California 94592

U.S. Navy Underwater Sound Ref. Lab.
Office of Naval Research
P.O. Box 8337
Orlando, Florida 32806

Chief of Naval Operations
Dept. of the Navy
Washington, D.C. 20350
Attn: Code Op07T

Strategic Systems Project Off.
Department of the Navy
Washington, D.C. 20390
Attn: NSP- 001 Chief Scientist

Deep Submergance Systems
Naval Ship Systems Command
Code 39522
Department of the Navy
Washington, D.C. 203 60

Engineering Dept.
U.S. Naval Academy
Annapolis, Maryland 21402

Naval Air Systems Command
Dept. of the Navy
Washington, D.C. 20360
Attn: NAVAIR 5302 Aero & Struc.
5308 Struc.
52031F Materials
604 Tech. Lib.

Director, Aero Mechanics
Naval Air Development Center
Johnsville
Warminster, Pennsylvania 18974

Technical Director
U.S. naval Undersea R&D Center
San Diego, California 92132

Engineering Department
U.S. Naval Academy
Annapolis, Maryland 21402

Naval Facilities Engineering Command
Dept. of the Navy
Washington, D.C. 20360
Attn: NAVFAC 03 Res. & Dev.
04 Res. & Dev.
14114 Tech. Lib.

Naval Sea Systems Command
Dept. of the Navy
Washington, D.C. 20360
Attn: NAVSHIP 03 Res. & Tech.
031 Ch.Scientist R&D
03412 Hydromechanics
037 Ship Silencing Div.
035 Weapons Dynamics

Navy cont.

Naval Ship Engineering Center
Prince George's Plaza
Hyattsville, Maryland 20782
Attn: NAVSEC 6100 Ship Sys Engr & Des Dep
6102C Computer-Aided Ship Des
6105G
6110 Ship Concept Des
6120 Hull Div.
6120D Hull Div.
6128 Surface Ship Struct.
6129 Submarine Struct.

Air Force

Commander WADD
Wright-Patterson Air Force Base
Dayton, Ohio 45433
Attn: Code WWRMDD
AFFDL (FDDS)
Structures Division
AFLC (MCEEA)

Chief, Applied Mechanics Group
U.S. Air Force Inst. of Tech.
Wright-Patterson Air Force Base
Dayton, Ohio 45433

Chief, Civil Engineering Branch
WLRC, Research Division
Air Force Weapons Laboratory
Kirtland AFB, New Mexico 87117

Air Force Office of Scientific Research
1400 Wilson Blvd.
Arlington, Virginia 22209
Attn: Mechanics Div.

NASA

Structures Research Division
National Aeronautics & Space Admin.
Langley Research Center
Langley Station
Hampton, Virginia 23365

National Aeronautic & Space Admin.
Associate Administrator for Advanced Research & Technology
Washington, D.C. 02546

Scientific & Tech. Info. Facility
NASA Representative (S-AK/DL)
P.O. Box 5700
Bethesda, Maryland 20014

Other Government Activities

Commandant
Chief, Testing & Development Div.
U.S. Coast Guard
1300 E. Street, N.W.
Washington, D.C. 20226

Technical Director
Marine Corps Dev & Educ. Command
Quantico, Virginia 22134

Director
National Bureau of Standards
Washington, D.C. 20234
Attn: Mr. B.L. Wilson, EN 219

Dr. M. Gaus
National Science Foundation
Engineering Division
Washington, D.C. 20550

Science & Tech. Division
Library of Congress
Washington, D.C. 20540

Director
Defense Nuclear Agency
Washington, D.C. 20305
Attn: SPSS

Commander Field Command
Defense Nuclear Agency
Sandia Base
Albuquerque, New Mexico 87115

Director Defense Research & Engr
Technical Library
Room 3C-128
The Pentagon
Washington, D.C. 20301

Chief, Airframe & Equipment Branch
FS-120
Office of Flight Standards
Federal Aviation Agency
Washington, D.C. 20553

Chief, Research and Development
Maritime Administration
Washington, D.C. 20235

Deputy Chief, Office of Ship Constr.
Maritime Administration
Washington, D.C. 20235
Attn: Mr. U.L. Russo

Atomic Energy Commission
Div. of Reactor Devel. & Tech.
Germantown, Maryland 20767

Ship Hull Research Committee
National Research Council
National Academy of Sciences
2101 Constitution Avenue
Washington, D.C. 20418
Attn: Mr. A.R. Lytle

Part 2 - Contractors and Other Technical Collaborators

Universities

Dr. J. Tinsley Oden
University of Texas at Austin
345 Eng. Science Bldg.
Austin, Texas 78712

Prof. Julius Miklowitz
California Institute of Technology
Div. of Engineering & Applied Sci.
Pasadena, California 91109

Dr. Harold Liebowitz, Dean
School of Engr. & Applied Science
George Washington University
725 - 23rd St., N.W.
Washington, D.C. 20006

Prof. Eli Sternberg
California Institute of Technology
Div. of Engr. & Applied Sciences
Pasadena, California 91109

Prof. Paul M. Naghdi
University of California
Div. of Applied Mechanics
Etcheverry Hall
Berkeley, California 94720

Professor P.S. Symonds
Brown University
Division of Engineering
Providence, R.I. 02912

Prof. A.J. Durelli
John F. Dodge Professor
Oakland University
Rochester, Michigan 48063

Prof. R.B. Testa
Columbia University
Dept. of Civil Engineering
S.W. Mudd Bldg.
New York, New York 10027

Prof. H.H. Bleich
Columbia University
Dept. of Civil Engineering
Amsterdam & 120th St.
New York, New York 10027

Prof. F.L. DiMaggio
Columbia University
Dept. of Civil Engineering
616 Mudd Building
New York, New York 10027

Prof. A.M. Freudenthal
George Washington University
School of Engineering & Applied Science
Washington, D.C. 20006

D.C. Evans
University of Utah
Computer Science Division
Salt Lake City, Utah 84112

Prof. Norman Jones
Massachusetts Inst. of Technology
Dept. of Naval Architecture & Marine Engrng
Cambridge, Massachusetts 02139

Asst. to Secretary Defense
Atomic Energy-Att. D. Cotter
Washington, D.C. 20301

Dr. V.R. Hodgson
Wayne State University
School of Medicine
Detroit, Michigan 48202

Universities cont.

Dean B.A. Boley
Northwestern University
Technological Institute
2145 Sheridan Road
Evanston, Illinois 60201

Prof. P.G. Hodge, Jr.
University of Minnesota
Dept. of Aerospace Engng & Mech.
Minneapolis, Minnesota 55455

Dr. D.C. Drucker
University of Illinois
Dean of Engineering
Urbana, Illinois 61801

Prof. N.M. Newmark
University of Illinois
Dept. of Civil Engineering
Urbana, Illinois 61801

Prof. E. Reissner
University of California, San Diego
Dept. of Applied Mechanics
La Jolla, California 92037

Prof. William A. Nash
University of Massachusetts
Dept. of Mechanics & Aerospace Eng.
Amherst, Massachusetts 01002

Library (Code 0384)
U.S. Naval Postgraduate School
Monterey, California 93940

Prof. Arnold Allentuch
Newark College of Engineering
Dept. of Mechanical Engineering
323 High Street
Newark, New Jersey 07102

Dr. George Herrmann
Stanford University
Dept. of Applied Mechanics
Stanford, California 94305

Prof. J.D. Achenbach
Northwestern University
Dept. of Civil Engineering
Evanston, Illinois 60201

Director, Applied Research Lab.
Pennsylvania State University
P.O. Box 30
State College, Pennsylvania 16801

Prof. Eugen J. Skudrzyk
Pennsylvania State University
Applied Research Laboratory
Dept. of Physics - P.O. Box 30
State College, Pennsylvania 16801

Prof. J. Kempner
Polytechnic Institute of Brooklyn
Dept. of Aero. Engrg & Applied Mech.
333 Jay Street
Brooklyn, N.Y. 11201

Prof. J. Klosner
Polytechnic Institute of Brooklyn
Dept. of Aerospace & Appl. Mech.
333 Jay Street
Brooklyn, N.Y. 11201

Prof. R.A. Schapery
Texas A&M University
Dept. of Civil Engineering
College Station, Texas 77840

Prof. W.D. Pilkey
University of Virginia
Dept. of Aerospace Engineering
Charlottesville, Virginia 22903

Dr. H.G. Schaeffer
University of Maryland
Aerospace Engineering Dept.
College Park, Maryland 20742

Prof. K.D. Willmert
Clarkson College of Technology
Dept. of Mechanical Engineering
Potsdam, N.Y. 13676

Dr. J.A. Stricklin
Texas A&M University
Aerospace Engineering Dept.
College Station, Texas 77843

Dr. L.A. Schmit
University of California, LA
School of Engineering & Applied Sci.
Los Angeles, California 90024

Dr. H.A. Kamel
The University of Arizona
Aerospace & Mech. Engineering Dept.
Tucson, Arizona 85721

Dr. B.S. Berger
University of Maryland
Dept. of Mechanical Engineering
College Park, Maryland 20742

Prof. G.R. Irwin
Dept. of Mechanical Engng.
University of Maryland
College Park, Maryland 20742

Dr. S.J. Fenves
Carnegie-Mellon University
Dept. of Civil Engineering
Schenley Park
Pittsburgh, Pennsylvania 15213

Dr. Ronald L. Huston
Dept. of Engineering Analysis
Mail Box 112
University of Cincinnati
Cincinnati, Ohio 45221

Prof. George Sih
Dept. of Mechanics
Lehigh University
Bethlehem, Pennsylvania 18015

Prof. A.S. Kobayashi
University of Washington
Dept. of Mechanical Engineering
Seattle, Washington 98105

Librarian
Webb Institute of Naval Architecture
Crescent Beach Road, Glen Cove
Long Island, New York 11542

Prof. Daniel Frederick
Virginia Polytechnic Institute
Dept. of Engineering Mechanics
Blacksburg, Virginia 24061

Prof. A.C. Eringen
Dept. of Aerospace & Mech. Sciences
Princeton University
Princeton, New Jersey 08540

Dr. S.L. Koh
School of Aero., Astro. & Eng. Sc.
Purdue University
Lafayette, Indiana 47907

Prof. E.H. Lee
Div. of Engrg. Mechanics
Stanford University
Stanford, California 94305

Prof. R.D. Mindlin
Dept. of Civil Engrg
Columbia University
S.W. Mudd Building
New York, N.Y. 10027

Prof. S.B. Dong
University of California
Dept. of Mechanics
Los Angeles, California 90024

Prof. Burt Paul
University of Pennsylvania
Towne School of Civil & Mech Engr
Rm. 113 - Towne Building
220 S. 33rd Street
Philadelphia, Pennsylvania 19104

Prof. J.W. Liu
Dept. of Chemical Engr. & Metal.
Syracuse University
Syracuse, N.Y. 13210

Prof. S. Bodner
Technion R&D Foundation
Haifa, Israel

Prof. R.J.H. Bollard
Chairman, Aeronautical Engr. Dept.
207 Guggenheim Hall
University of Washington
Seattle, Washington 98105

Prof. G.S. Heller
Division of Engineering
Brown University
Providence, Rhode Island 02912

Prof. Werner Goldsmith
Dept. of Mechanical Engineering
Div. of Applied Mechanics
University of California
Berkeley, California 94720

Prof. J.R. Rice
Division of Engineering
Brown University
Providence, R.I. 02912

Prof. R.S. Rivlin
Center for the Application of
Mathematics
Lehigh University
Bethlehem, Pennsylvania 18015

Bell Telephone Labs Inc.
505 King Avenue -Tech. Lib.
Columbus, OH 43201

Dr. Francis Cozzarelli
Div. of Interdisciplinary
Studies & Research
School of Engineering
State University of New York
Buffalo, N.Y. 14214

Industry and Research Institutes

Library Services Dept.
Report Section Bldg. 14-14
Argonne National Laboratory
9700 S. Cass Avenue
Argonne, Illinois 60440

Dr. M.C. Junger
Cambridge Acoustical Associates
129 Mount Auburn St.
Cambridge, Massachusetts 02138

Dr. L.H. Chen
General Dynamics Corporation
Electric Boat Division
Groton, Connecticut 06340

Dr. J.E. Greenspon
J.G. Engineering Research Assoc.
3831 Menlo Drive
Baltimore, Maryland 21215

Dr. S. Batdorf
The Aerospace Corp.
P.O. Box 92957
Los Angeles, California 90009

Dr. K.C. Park
Lockheed Palo Alto Research Lab.
Dept. 5233, Bldg. 205
3251 Hanover St.
Palo Alto, CA 94304

Library
Newport News Shipbuilding & Dry
Dock Company
Newport News, Virginia 23607

Dr. W.F. Bozich
McDonnell Douglas Corporation
5301 Bolsa Avenue
Huntington Beach, CA 92647

Dr. H.N. Abramson
Southwest Research Institute
Technical Vice President
Mechanical Sciences
P.O. Drawer 28510
San Antonio, Texas 78284

Dr. R.C. DeHart
Southwest Research Institute
Dept. of Structural Research
P.O. Drawer 28510
San Antonio, Texas 78284

Dr. M.L. Baron
Weidlinger Associates, Consulting
Engineers
110 East 59th Street
New York, N.Y. 10022

Dr. W.A. Von Riesmann
Sandia Laboratories
Sandia Base
Albuquerque, New Mexico 87115

Dr. T.L. Geers
Lockheed Missiles & Space Co.
Palo Alto Research Laboratory
3251 Hanover Street
Palo Alto, California 94304

Dr. J.L. Tocher
Boeing Computer Services, Inc.
P.O. Box 24346
Seattle, Washington 98124

Mr. William Caywood
Code BBE, Applied Physics Laboratory
8621 Georgia Avenue
Silver Spring, Maryland 20034

Mr. P.C. Durup
Lockheed-California Company
Aeromechanics Dept., 74-43
Burbank, California 91503

Assistant Chief for Technology
Office of Naval Research, Code 200
Arlington, Virginia 22217

Los Alamos Scientific Lab
P.O. Box 1663 - Tech Labs
Los Alamos, NM 87544

Boeing Company
Attn. Aerospace Lab
P.O. Box 3707
Seattle, WA 98124

IIT Research Institute
10 West 35th Street
Chicago, ILL 60616

Unclassified

SECURITY CLASSIFICATION OF THIS PAGE (When Data Entered)

REPORT DOCUMENTATION PAGE

READ INSTRUCTIONS BEFORE COMPLETING FORM

1. REPORT NUMBER: 46	2. GOVT ACCESSION NO.
3. RECIPIENT'S CATALOG NUMBER	
4. TITLE (and Subtitle): OPTIMIZATION OF GEOMETRIC DISCONTINUITIES IN STRESS FIELDS	5. TYPE OF REPORT & PERIOD COVERED: Technical Report
6. PERFORMING ORG. REPORT NUMBER	
7. AUTHOR(s): A. J. Durelli, K. Brown, P. Yee	8. CONTRACT OR GRANT NUMBER(s): N0014-76-C-0487
9. PERFORMING ORGANIZATION NAME AND ADDRESS: Oakland University, Rochester, MI 48063	10. PROGRAM ELEMENT, PROJECT, TASK AREA & WORK UNIT NUMBERS
11. CONTROLLING OFFICE NAME AND ADDRESS: Office of Naval Research, Department of the Navy, Washington, D.C. 20025	12. REPORT DATE: Mar 78
	13. NUMBER OF PAGES: ~~36~~ 32 pp
14. MONITORING AGENCY NAME & ADDRESS(if different from Controlling Office)	15. SECURITY CLASS. (of this report): Unclassified
	15a. DECLASSIFICATION/DOWNGRADING SCHEDULE

16. DISTRIBUTION STATEMENT (of this Report)

Distribution of this report is unlimited

17. DISTRIBUTION STATEMENT (of the abstract entered in Block 20, if different from Report)

18. SUPPLEMENTARY NOTES

19. KEY WORDS (Continue on reverse side if necessary and identify by block number)

Optimization
Photoelasticity
Ideal Fillets
Stress Concentrations
Weight Saving

20. ABSTRACT (Continue on reverse side if necessary and identify by block number)

The ideal boundary of a discontinuity is defined as that boundary along which there is no stress concentration. Photoelastically an isochromatic coincides with the ideal boundary. This property is used to develop experimentally ideal boundaries for some cases of technological interest. The concept of 'coefficient of efficiency' is introduced to evaluate the degree of optimization. The procedure to idealize boundaries is illustrated for the two cases of the circular tube and of the perforated rectangular plate, with

→over

DD FORM 1 JAN 73 1473 EDITION OF 1 NOV 65 IS OBSOLETE
S/N 0102-014-6601

SECURITY CLASSIFICATION OF THIS PAGE (When Data Entered)

405 252

prescribed functional restraints and a particular criterion for failure. An ideal design of the inside boundary of the tube is developed which decreases its maximum stress by 25%, at the time it also decreases its weight by 10%. The efficiency coefficient is increased from 0.59 to 0.95. Tests with a brittle material show an increase in strength of 20%. An ideal design of the boundary of the hole in the plate reduces the maximum stresses by 26% and increases the coefficient of efficiency from 0.54 to 0.90.